EPJ Web of Conferences **125**, 01001 (2016) DOI: 10.1051/epjconf/201612501001
QUARKS-2016

Recent results from CMS

Milos Dordevic[1] on behalf of the CMS Collaboration ⋆

[1] *Vinca Institute of Nuclear Sciences, PO Box 522, 11001 Belgrade, Serbia*

Abstract. The highlights of the most recent CMS results with 13 TeV data will be presented in this overview. The Standard Model precision measurements, including the top quark production, will be shown first. This will be followed by the presentation of Higgs boson studies with the early 13 TeV data. Then the focus will shift to searches for physics beyond the Standard Model, including the searches for several Supersymmetric scenarios, using different analysis techniques. The talk will conclude with searches for the exotic resonances, with an emphasis on studies of the high-mass diphoton production.

1 Introduction

The LHC Run I was very successful for the CMS Collaboration, with the major event being the discovery of the Higgs boson. A large number of studies of the known processes and searches for new phenomena was conducted, all of them confirming the prediction of the Standard Model (SM) with the unprecedented precision. The first studies of 13 TeV data recorded by the CMS experiment in the year of 2015 will be presented in this overview.

2 Standard Model results at 13 TeV

2.1 Studies of two-particle correlations

The two-particle angular correlations for charged particles are studied at 13 TeV [1]. The presence of the ridge-like structure for long range ($|\eta| > 2.0$) near-side $\Delta\phi \approx 0$ pairs is confirmed, as shown in Fig. 1. The magnitude of the correlation is maximal in the range $1.0 < p_T < 2.0$ GeV/c, with an approximately linear increase with the charge particle multiplicity, similar to the one measured at the 7 TeV [2], but now extended to much higher multiplicity values. Strong collision system size dependence is observed when comparing data from pp, pPb and PbPb collisions.

2.2 W and Z boson production

Total inclusive and fiducial W and Z boson cross sections at 13 TeV are measured in electron and muon final states [3]. The total inclusive cross sections times branching fractions are $\sigma(pp \to W^+X \times B(W^+ \to l^+\nu) = 11370 \pm 50(stat) \pm 230(syst) \pm 550(lumi)pb$, $\sigma(pp \to W^-X \times B(W^- \to l^-\nu) = 8580 \pm 50(stat) \pm 160(syst) \pm 410(lumi)pb$ and $\sigma(pp \to ZX \times B(Z \to l^+l^-) = 1910 \pm 10(stat) \pm$

⋆e-mail: milos.dordevic@cern.ch

$40(syst) \pm 90(lumi)pb$ for the dilepton mass range of 60 to 120 GeV. The measured ratio of the W and Z boson cross section in the electron and muon channels, that is useful also as an additional check of the lepton universality, is shown in Fig. 2. The measurement is found to be in a good agreement with the SM prediction.

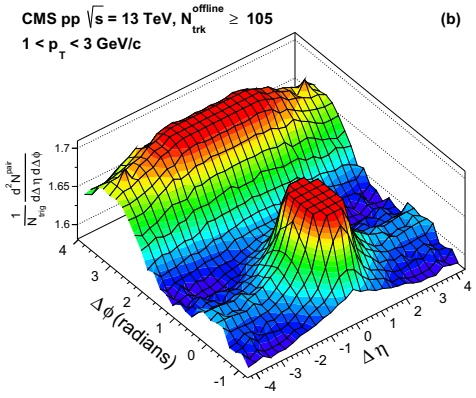

Figure 1. The two-particle correlation function for pairs of charge particles both in range 1 < p_T <3 GeV/c, showing the "rigde"-like structure.

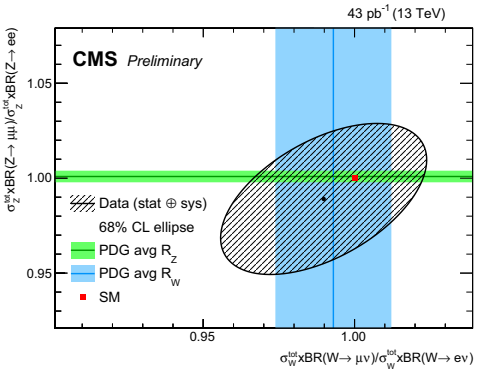

Figure 2. Ratios of W and Z inclusive cross sections in the electron and muon channels, as test of lepton universality and the SM expectation.

2.3 Inclusive jet production

Double-differential inclusive jet cross section, as a function of jet transverse momentum and rapidity, is measured for two jet size parameters R=0.7 and R=0.4 and jets with p_T up to 2 TeV and $|y|$ = 4.7 [4] and the results are presented in Fig. 3. The new energy of 13 TeV provides an access to kinematic region of momentum fraction x where the parton density is large. When comparing the data to predictions at NLO accuracy in pQCD, a better agreement is observed for the larger jet size. The NLO prediction matched to parton shower from POWHEG+PYTHIA8 [5, 6] performs equally well for the both jet cone size parameters. The LO predictions of PYTHIA8 and HERWIG++ [7] have significant discrepancies with respect to data, thus stressing the importance of the higher order corrections.

2.4 Single top production

The top quark mass was measured in single top events [8], where the W boson decays to muon and a neutrino. Specific event topology and kinematics, featuring the central production of a light jet and an asymmetry of the initial state, was exploited to suppress the ttbar background. The measured value of $m_t = 172.60 \pm 0.77(stat)^{+0.97}_{-0.93}(syst)$ GeV, extracted from a fit to the top mass distribution (Fig. 4), is in a good agreement with the world average of $m_t = 173.34 \pm 0.76$ GeV. The t-channel single top cross section at 13 TeV is measured as well [9]. Kinematic variables are combined into a multivariate discriminator that was fit to obtain the inclusive cross section of $\sigma_{t-ch.} = 227.8 \pm 9.1(stat.) \pm 14.0(exp.)^{+28.7}_{-27.7}(theo.) \pm 6.2(lumi.)pb = 227.8^{+33.7}_{-33.0}pb$, found to be in a good agreement with the SM expectation.

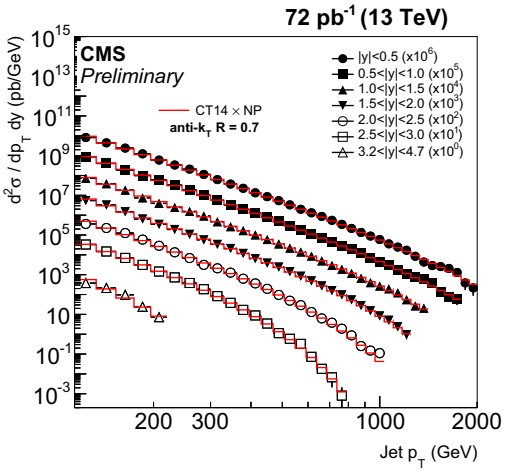

Figure 3. Double-differential inclusive jet cross section, shown as a function of the jet transverse momentum.

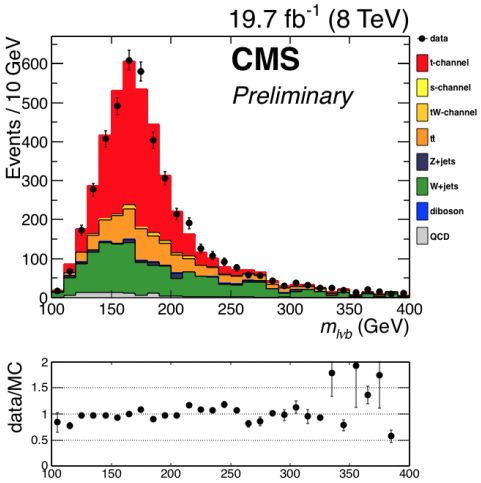

Figure 4. The top quark mass after the final selection including also the charge and pseudorapidity cuts.

3 Higgs studies at the 13 TeV

3.1 ttH production

A search for SM Higgs boson in association with a top quark pair at 13 TeV is performed. The analysis targets the bbar, $\gamma\gamma$ and multilepton decays of the Higgs boson. The multilepton analysis selects final states with two same-sign leptons or more than three leptons produced in association with b jets [10]. The signal extraction is based on the two-dimensional multivariate discriminator trained against each of the ttbar and ttV backgrounds, as shown in Fig. 5. The signal strenght is measured to be the $0.6^{+1.4}_{-1.1}$ times the SM expectation and the observed (expected) 95% CL limits are 3.3 (2.6) times the SM expectation. For the Higgs boson decays to a pair of b quarks, the lepton plus jets and dileptonic decays of the ttbar system are considered [11]. A combination of the matrix element method and multivariate approach is performed. A combined fit of the multivariate discriminant templates to data yielded with the signal strength of $-2.0^{+1.8}_{-1.8}$ and the observed (expected) 95% CL limits are 2.6 (3.6) times the SM expectation. The Higgs to diphotons analysis, although statistically limited at this point, was performed with the inclusion of the two categories with leptonic and hadronic tags of the ttbar pair [12]. The signal strength for the ttH production in this channel is $-3.8^{+4.5}_{-3.6}$, with the two tags corresponding to the ttH process combined statistically.

3.2 Higgs decays to bosons

The diphoton channel remains one of the best to test Higgs properties. It was performed in the gg→H, VBF and ttH categories [12]. Small deficit that is observed is driven by the untagged categories (gg→H). The observed (expected) significance at 125.09 GeV is 1.7(2.7)σ and the signal strength of $0.69^{+0.47}_{-0.42}$ is consistent with the SM expectation, as shown in Fig. 7. The H→ZZ→4l analysis, based on the matrix element kinematic discriminant between signal and background, is performed [13]. The distribution of the four lepton invariant mass is shown in Fig. 8. The observed(expected) significance

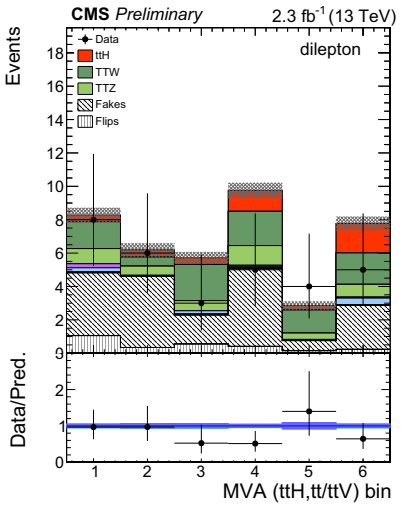

Figure 5. BDT kinematic discriminant for signal extraction in two same-sign lepton category.

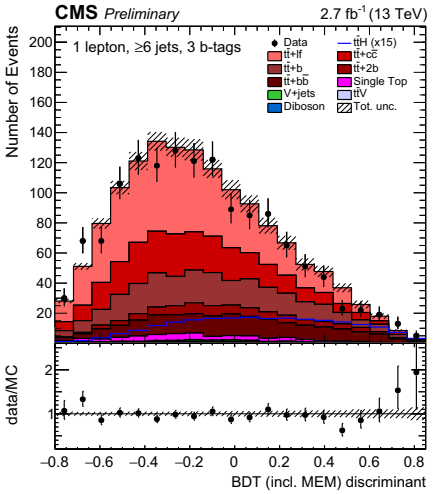

Figure 6. Final discriminator shape of the BDT, including also the MEM discriminator in the training.

at 125.09 GeV of 2.5(3.4)σ and the signal strength of $0.82^{+0.57}_{-0.43}$ are consistent with the SM within the uncertainties.

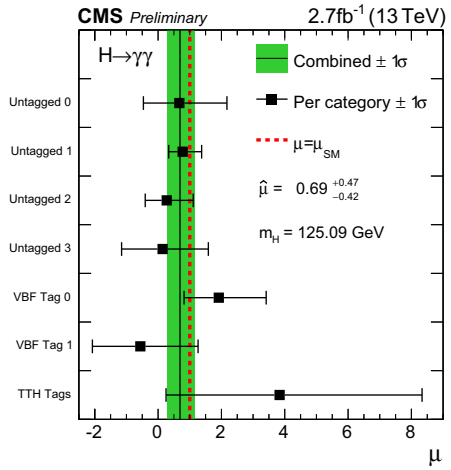

Figure 7. Signal strength modifier for each category in H→ $\gamma\gamma$ channel, compared to the overall signal strength and to the SM expectation.

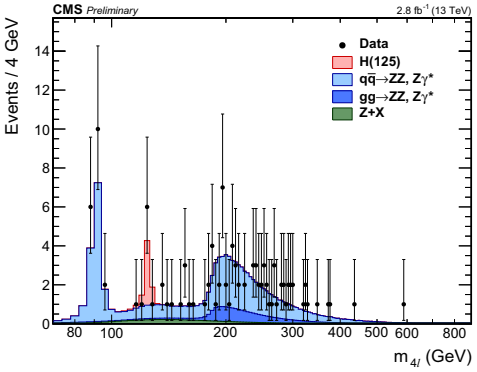

Figure 8. The four lepton invariant mass distribution m_{4l}, shown in the full studied mass range.

4 Supersymmetry searches at the 13 TeV

4.1 SUSY with zero leptons

The searches for gluino pair production with the LSP and zero leptons in the final state are performed [14]. The results of the analysis using the HT variables, as shown in Fig. 9, provides some of the world leading limits on T1bbbb, T1tttt and T1qqqq of 1600, 1530 and 1440 GeV. Similar search was performed using the stransverse mass variable M_{T2}, which is a measure of the transverse momentum imbalance in an event [15]. No excess above the SM background is observed and gluino(neutralino) mass was probed up to 1725(1100) GeV, as shown in Fig. 10, extending the Run 1 sensitivity by more than 300 GeV [16].

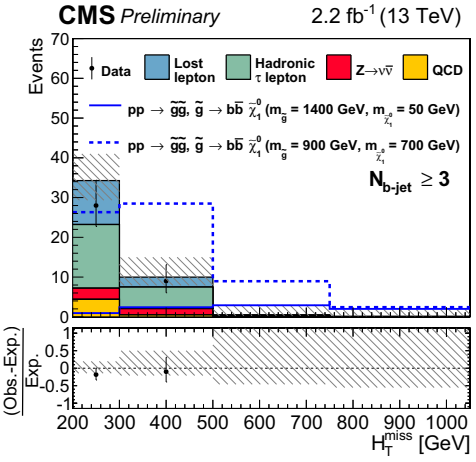

Figure 9. Observed number of events and SM background predictions for one of the search regions sensitive to the T1bbbb scenarios.

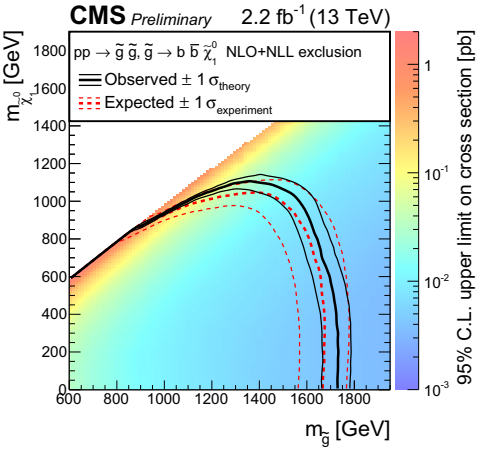

Figure 10. Exclusion limit at 95% CL for gluino mediated bottom-squark production.

4.2 SUSY with one lepton

The zero lepton SUSY search using the Razor variables is extended with an additional one lepton category [17]. The events are further categorised by the number of b-tagged jets in the final state. For the 100 GeV neutralino mass and gluino decaying to bb pairs, the limits are set to 1650 GeV, while for the decays to top(light) quarks this particular SUSY scenario is excluded up to 1600(1350) GeV, as shown in Fig. 11. The search for SUSY in final state with one lepton, one b-tagged jet and large missing transverse energy (MET) was performed using the sum of masses of large radius jets [18]. A key feature of this analysis is that the dominant background ttbar is nearly uncorrelated with the transverse mass of the lepton and MET. The distribution of the M_J variable is shown in Fig. 11. Within the T1tttt scenario the gluino mass is excluded up to 1575 GeV.

5 Exotica searches at the 13 TeV

5.1 Search for black holes

The search for black holes is performed [19] in the framework of ADD model with n-extra dimensions [20–22]. The semiclassical and quantum black holes are considered. The SM background, dominated

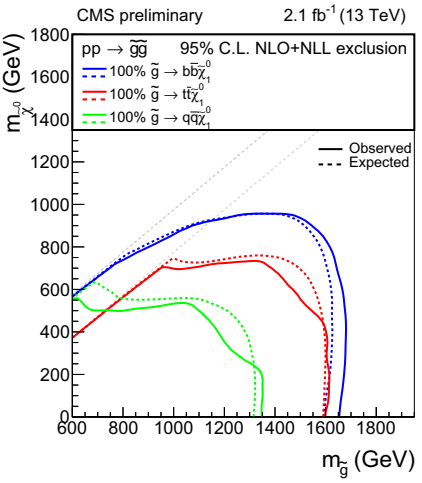

Figure 11. Summary of the exclusion contours at 95% CL, with gluino decays at 100% branching fraction to LSP and bb, tt and qq pairs.

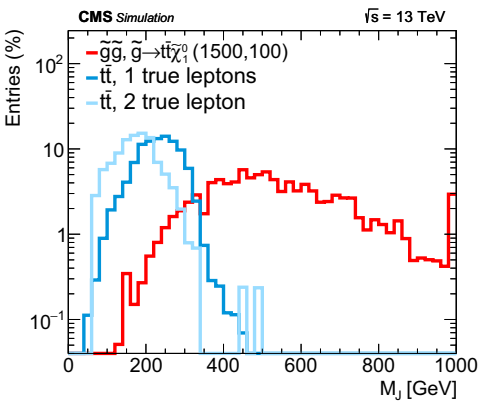

Figure 12. Distribution of M_J from simulated events with a small amount of initial state radiation (ISR).

by the QCD multijet events, is estimated from data. The distribution of the discriminating variable S_T, representing a scalar sum of the transverse energies of all energetic objects in the event, is shown in Fig. 13. No significant excess has been observed and the 95% CL limits in the semiclassical(quantum) black hole interpretation of 8.7(8.0) TeV are established. These limits are surpassing the 8 TeV results of 5.5 - 6.0 TeV [23].

5.2 Search for dark matter

The search for dark matter in the final state with large MET and at least one jet with high transverse momentum is performed [24]. The dark matter is considered to be produced in pairs, via the decay of a vector mediator, and the signal is extracted from a fit to the observed MET distribution in data. The mediator mass up to 1.3 TeV is excluded at 90% CL, as it is shown in Fig. 14 where also the results from the other, non-collider experiments, are overlaid together with this measurement, for the comparison.

5.3 Search for diphoton resonances

The search for diphoton resonances, under the 2HDM (spin 0) or ADD/RS (spin 2) hypothesis, is performed [25]. The high diphoton mass region between the 500 GeV and 4.5 TeV is explored, with the relative width up to 5.6×10^{-2}. The 13 TeV results are combined with similar searches at the 8 TeV [26, 27]. The largest excess is observed at 750 GeV and resonance width of 1.4×10^{-4}, with the local p-value of 3.4σ, reduced to 1.6σ when taking into account of searching for the several signal hypotheses. The corresponding diphoton mass distribution and p-value are shown in Fig. 15 and Fig. 16, respectively.

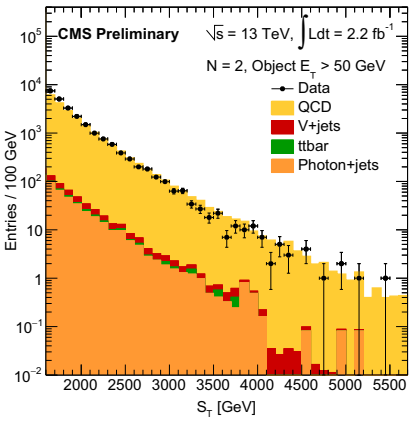

Figure 13. The S_T variable distribution, with the main contribution from QCD multijet background.

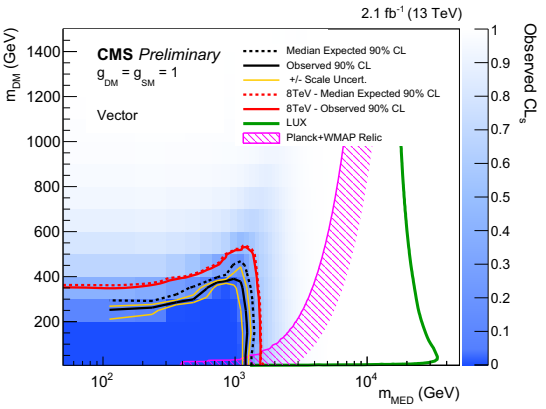

Figure 14. The dark matter exclusion contours in the $m_{med} - m_{DM}$ plane assuming a vector-type interaction.

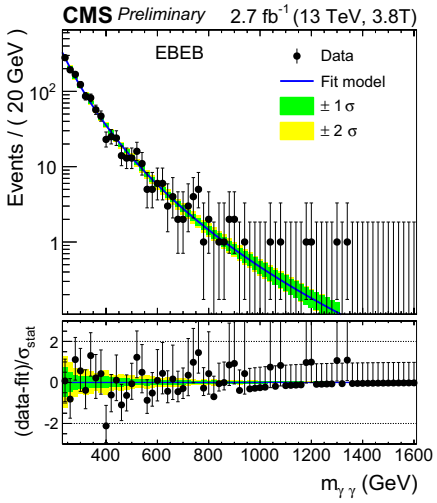

Figure 15. The observed invariant mass spectra for the EBEB channel and using the 3.8T dataset.

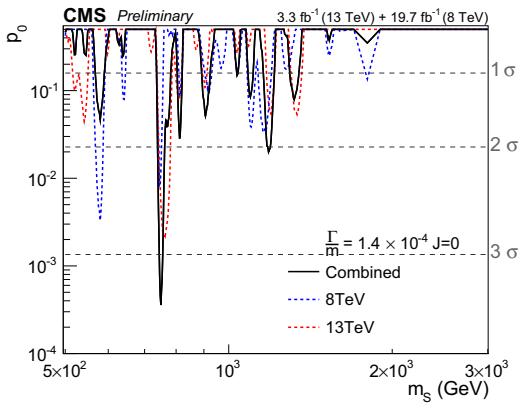

Figure 16. The observed background only p-values for spin 0 and the most narrow width hypothesis, obtained from the combination of the 8 and 13 TeV results.

6 Conclusion

The 2015 has marked a start of CMS taking the 13 TeV data. It was the first operation under the 25ns conditions and physics objects are well commissioned. The SM results are generally in an agreement with the prediction, many new physics results have an improved sensitivity and an excess in the diphoton invariant mass is observed at 750 GeV, that requires more data for a precise scrutiny of its existence.

References

[1] The CMS Collaboration, Phys. Rev. Lett. 116, 172302, (2016)
[2] The CMS Collaboration, JHEP **09** 091, (2016)
[3] The CMS Collaboration, CMS-PAS-SMP-15-004, (2016)
[4] The CMS Collaboration, CMS-PAS-SMP-15-007, (2016)
[5] T. Sjostrand, S. Mrenna and P. Skands, JHEP **05** 026, (2006)
[6] T. Sjostrand, S. Mrenna and P. Skands, Comput. Phys. Comm. **178** 852, (2008)
[7] G. Corcella et al., JHEP **0101** 010, (2001)
[8] The CMS Collaboration, CMS-PAS-TOP-15-001, (2016)
[9] The CMS Collaboration, CMS-PAS-TOP-16-003, (2016)
[10] The CMS Collaboration, CMS-PAS-HIG-15-008 (2016)
[11] The CMS Collaboration, CMS-PAS-HIG-16-004, (2016)
[12] The CMS Collaboration, CMS-PAS-HIG-15-005, (2016)
[13] The CMS Collaboration, CMS-PAS-HIG-15-004, (2016)
[14] The CMS Collaboration, CMS-PAS-SUS-15-002 (2016)
[15] The CMS Collaboration, CMS-PAS-SUS-15-003, (2016)
[16] The CMS Collaboration, JHEP **05** 078, (2015)
[17] The CMS Collaboration, CMS-PAS-SUS-15-004, (2016)
[18] The CMS Collaboration, CMS-PAS-SUS-15-007, (2016)
[19] The CMS Collaboration, CMS-PAS-EXO-15-007, (2016)
[20] N. Arkani-Hamed, S. Dimopoulos, G.R. Dvali, Phys. Lett. B **429** 264, (1988)
[21] N. Arkani-Hamed, S. Dimopoulos, G.R. Dvali, Phys. Lett. B **436** 257, (1988)
[22] N. Arkani-Hamed, S. Dimopoulos, G.R. Dvali, Phys. Rev. D **59** 086004, (1999)
[23] G. Landsberg, Fundam. Theor. Phys., **178** 267 (2015)
[24] The CMS Collaboration, CMS-PAS-EXO-15-003, (2016)
[25] The CMS Collaboration, CMS-PAS-EXO-16-018, (2016)
[26] The CMS Collaboration, Phys. Lett **750** 494-419, (2016)
[27] The CMS Collaboration, CMS-PAS-EXO-12-045, (2016)